World Academy of Science, Engineering and Technology
International Journal of Structural and Construction Engineering
Vol:16, No:8, 2022

Local Mechanical Analysis of Arch Foot of Space Y-Beam Arch Bridge

Cao Ziyuan, Luo Xuan

Open Science Index, Structural and Construction Engineering Vol:16, No:8, 2022 publications.waset.org/10012619.pdf

***Abstract*—**To study the local force characteristics of a spatial Y-arch bridge, a medium-bearing spatial Y-arch bridge is used as the object of study, and the finite element software FEA is used to establish a spatial finite element model and analyze the force conditions of the arch legs under different most unfavorable loading conditions. It is found that the forces on the arch foot under different conditions are mainly in the longitudinal direction and transverse direction, which should be considered for strengthening. The research results can provide reference for the design and construction of the same type of bridge.

***Keywords*—**Bridge engineering, special-shaped arch bridge, mechanical properties, local analysis.

I. Introduction

THE special-shaped arch bridge has become an important type of bridges in cities and scenic spots in China, and has good application prospects. Although China' s special-shaped bridges started late, they developed rapidly. China has successively built special-shaped arch bridges such as Wuchazi Bridge and Jiulongjiang Bridge. It can be predicted that the construction of special-shaped arch bridges in China will enter a steady development period.

For the underpass arch bridge, the main beam is the key part of the structural stress. By establishing the finite element model of the main girder of the arch bridge and conducting local stress analysis, Xu et al. [1] found that the stress in the anchorage area is large and stress concentration occurs, and appropriate stiffening ribs should be added, which provides a design reference for the construction of the down-bearing arch bridge. To study whether the strength of the anchor head in the anchorage zone of the suspender node of the tied arch bridge meets the stress requirements, Shuirong et al. [2] took the real bridge as the background, designed a full-scale model and compared it with the finite element model. The stress concentration occurred at the contact between the stiffening plate of the double-layer steel sleeve and the steel cushion plate, which led to the local stress overrun of the stiffening plate, and the stiffening plate should be strengthened. Wang et al. [3] used the overall calculation and plate-shell finite element analysis to analyze the anchorage zone structure, and proposed the optimization scheme of the arch rib suspender anchorage structure. The lower part of the horizontal plate was transformed into a closed chamber through the steel plate, so that the stress of the whole plate of the tensile vertical plate and the bending horizontal plate was more uniform and reasonable, and the stress concentration was effectively reduced. Wenhua et al. [4] analyzed the mechanical properties of arch-beam joints of an inclined arch bridge under different working conditions, and considered that the cross position of arch-beam should be strengthened in design. Ruanbo [5] used finite element software ANSYS to analyze the model of the anchorage segment of the side arch rib tie rod of the bridge. It was found that there was a large main tensile stress at the edge of some sharp corners and the edge of the local compression zone of the bearing. The area with large steel structure stress appeared in the roof of the steel longitudinal beam. Liu [6] analyzed the spatial stress of the through steel box basket-lift arch bridge, and established a solid element model for local analysis of the arch foot. The results showed that the stress level of the end beam was small, and the stress concentration of the arch rib and the main beam web should be paid attention to. The research results can provide reference for the design of the same type of bridges. Ke et al. [7] took the cable arch and cable beam anchorage zone of the suspender arch bridge as the key node, carried out local refined finite element calculation and analysis on the cable arch and cable beam anchorage structure of the bridge, and the results showed that it met the specification requirements

The structural form of the arch bridge studied in this paper is not rigidly adhered to the traditional one. The main arch rib uses space Y-shaped structure. At the same time, the design idea of butterfly arch is adopted, and the auxiliary arch is added as the auxiliary bearing component. It has the characteristics of light system, simple structure and beautiful shape. The results and discussions are of engineering value.

II. Method

The calculation of the model adopts FEA, a large-scale finite element software. The concrete adopts 3D solid element, and the rib plate, the cushion plate and the bearing plate adopt 2D shell element. The slip between the arch foot, the arch rib concrete and the arch rib steel plate is not considered. In the modeling, the concrete and the arch rib steel plate are completely jointed. The concrete adopts 8-node hexahedral element, and the arch rib steel plate adopts 4-node 2D element. The ordinary reinforcement is not considered in the model.

The boundary conditions of the model are: the complete consolidation treatment at the bottom of the arch foot (shown in Fig. 1), that is, the displacement of the bottom node of the arch foot in X direction (longitudinal bridge direction), Y direction (transverse bridge direction), Z direction (vertical), where the

Cao Ziyuan* and Luo Xuan are with School of Highway, Chang'an University, Xi'an 710064, China (*e-mail: 2020121038@chd.edu.cn).

positive direction of the Y axis points to the upstream side of the Jing River.

Fig. 1 Finite Element Model for Local Analysis

The loading method is as follows: A main node is established at the centroid position of the arch rib end, and the node of the arch rib end section is a subordinate node. The master-slave constraint is established between the two nodes. The suspender forces S1 and S2 adopt the same loading method. The load (force and moment) corresponding to various combinations of working conditions in the Midas Civil bar system model is applied to the main node as the boundary load of the solid finite element model. The support reaction at the beam position is applied to the corresponding position in the form of uniform load, and the load area is the size of the support. The load is divided into two parts, one is the self-weight of the arch base and the steel arch, and the other is the force applied by the original structure at the local model section calculated by Midas Civil under three working conditions. Prestress is simulated by implantable truss/beam element type.

III. Result

For local structure calculation, two other load cases with constant load and large stress are adopted:

- working condition 1: Permanent load
- working condition 2: Long term effect combination
- working condition 3: Fundamental combination for action effects

The local analysis model load magnitudes are shown in Table I.

TABLE I
THE MOST UNFAVORABLE LOAD VALUE UNDER LOAD CONDITION COMBINATION
A

Loading condition	Major arch			Downstream side arch			Upstream side arch		
	Axial force (kN)	Shearing force -Y (kN)	Shearing force -Z (kN)	Axial force (kN)	shearing force -Y (kN)	shearing force -Z (kN)	axial force (kN)	shearing force -Y (kN)	shearing force -Z (kN)
1	-27556.4	0.7	-173.8	-3223.6	-9.5	22.7	-3226.5	9.8	22.9
2	-34424.6	-400.6	-800.7	-4820.8	-104.5	-23.6	-4919.9	-35.6	-18.4
3	-34273.3	-129.4	-1030.3	-5232.1	-48.6	-56.6	-4253.8	-19.4	-32.2

B

Loading condition	Major arch			Downstream side arch			Upstream side arch		
	Torsional moment (kN·m)	Bending moment -Y (kN·m)	Bending moment -Z (kN·m)	Torsional moment (kN·m)	Bending moment -Y (kN·m)	Bending moment -Z (kN·m)	Torsional moment (kN·m)	Bending moment -Y (kN·m)	Bending moment -Z (kN·m)
1	0.0	-5249.4	12.7	-87.0	-149.4	45.9	80.9	-152.5	-43.2
2	-1.9	-10677.4	-4540.8	-1101.4	-654.9	-430.7	-946.0	-780.2	-590.8
3	-2.2	-13744.8	-4956.3	-1331.2	-800.9	-724.7	-1147.4	-681.7	-830.9

C

Loading condition	S1 suspender force (kN)	S2 suspender force (kN)	Reaction force of downstream side support (kN)	The upstream side support reaction force (kN)
1	981.7	1137.5	-1838.8	-1841.4
2	950	1240	-3393.6	-3493.5
3	1122	1636.8	-4380.6	-4709.0

The arch shaft material is Q420qDNH and the arch base material is C40 concrete.

TABLE II
MAXIMUM TENSILE STRESS AND COMPRESSIVE STRESS OF ARCH RIB CONCRETE
A

Loading condition	Maximum compressive stress (design strength 19.1 MPa)				Position of appearance		Maximum overrun area
	Longitudinal Direction	Transverse Direction	Hill-and-dale	Main compressive stress P1	Longitudinal, horizontal and vertical directions	Main compressive stress P1	
1	-2.18	1.12	-1.63	-3.33	Position of lower part of interface between arch rib and concrete	Upper interface	Not exceeding the limit
2	-9.91	-5.57	-16.27	-3.38		Lower part of the interface	
3	-10.98	-6.32	-17.76	-4.53		Lower part of the interface	

Open Science Index, Structural and Construction Engineering Vol:16, No:8, 2022 publications.waset.org/10012619.pdf

B

Loading condition	Maximum tensile stress (design strength 1.71 MPa)				Position of appearance		Maximum overrun area
	Longitudinal direction	Transverse direction	Hill-and-dale	Main compressive stress P1	Longitudinal, horizontal and vertical directions	Main compressive stress P1	
1	0.18	0.79	0.41	0.84	The upper position of the interface between arch rib and concrete	Position of lower part of interface between arch rib and concrete	Not exceeding the limit
2	11.49	4.13	8.94	0.79			< 1.9%
3	11.94	4.19	9.38	1.17			< 0.9%

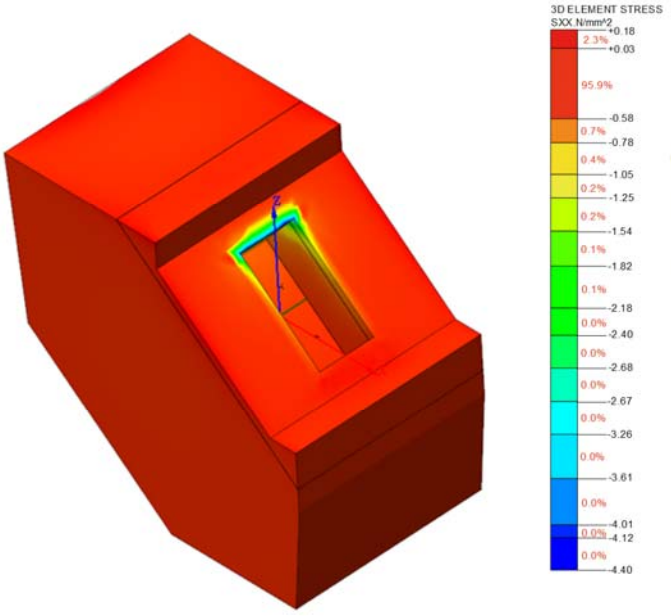

(a) Stress nephogram of longitudinal bridge

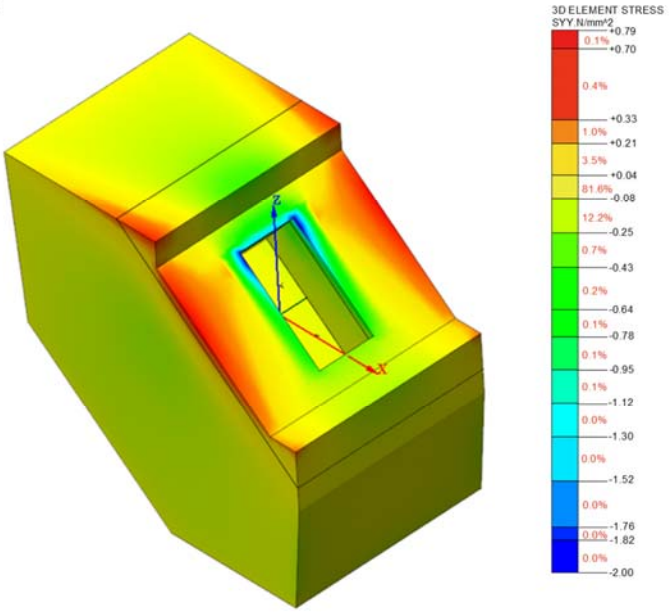

(b) Cross-bridge stress nephogram

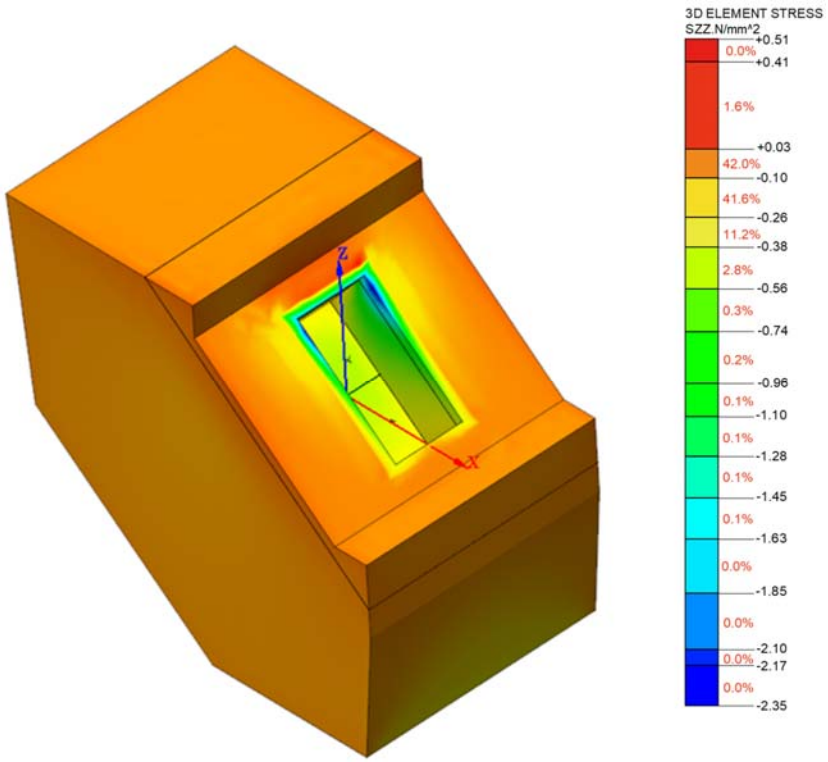

(c) Vertical stress nephogram

Fig. 2 Force of arch foot under working condition 1

Open Science Index, Structural and Construction Engineering Vol:16, No:8, 2022 publications.waset.org/10012619.pdf

Open Science Index, Structural and Construction Engineering Vol:16, No:8, 2022 publications.waset.org/10012619.pdf

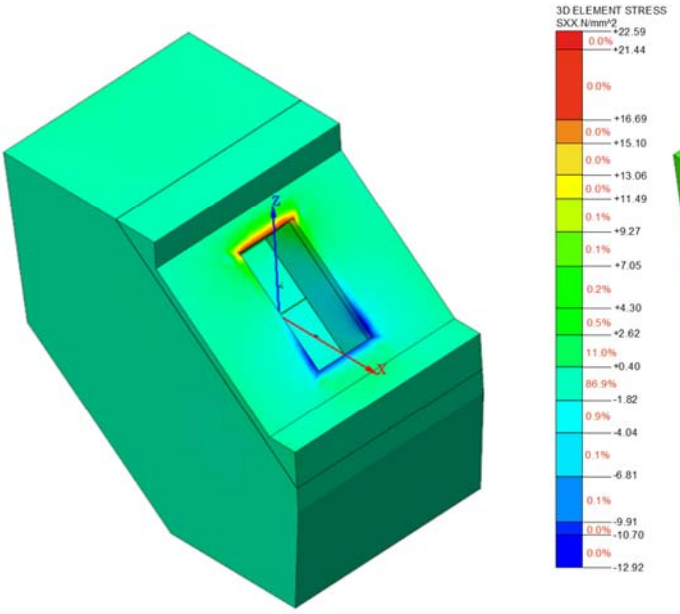

(a) Stress nephogram of longitudinal bridge

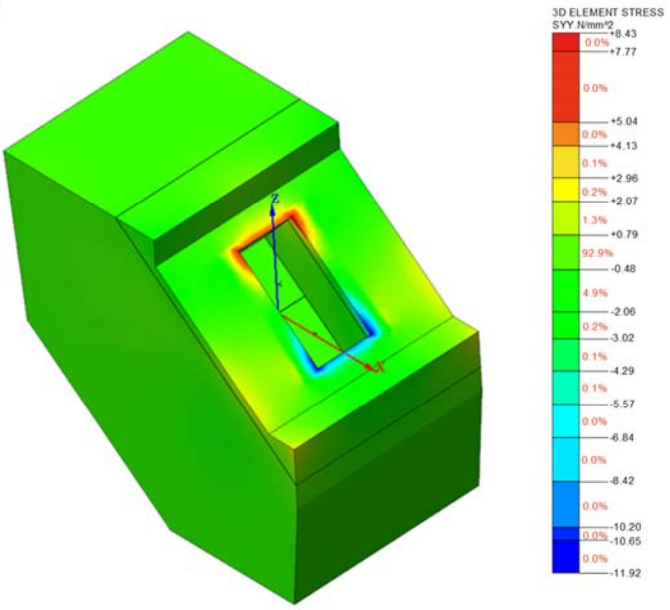

(b) Cross-bridge stress nephogram

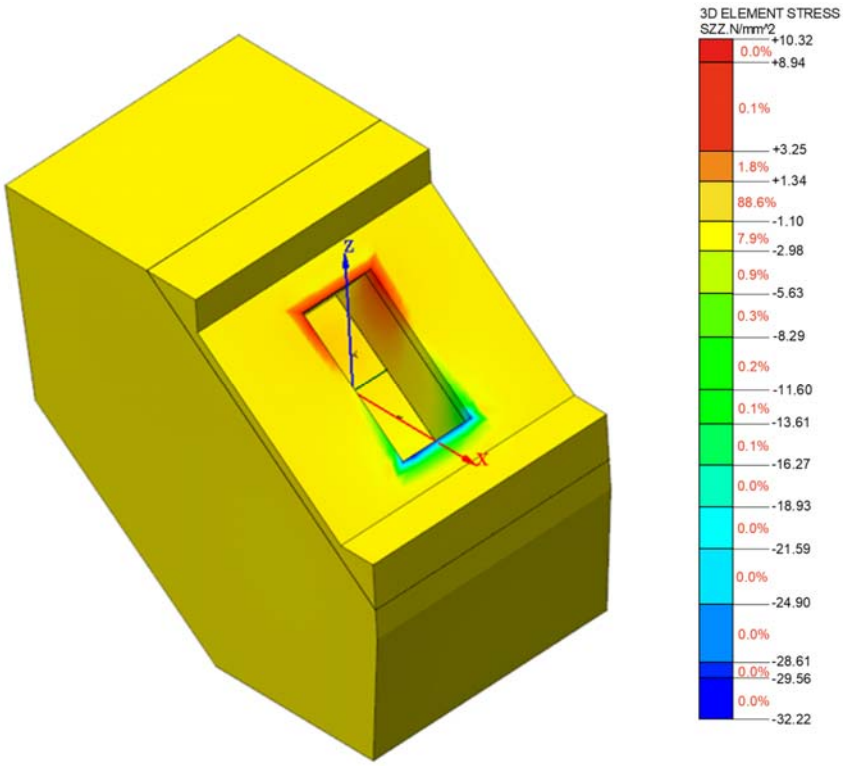

(c) Vertical stress nephogram

Fig. 3 Force of arch foot under working condition 2

Open Science Index, Structural and Construction Engineering Vol:16, No:8, 2022 publications.waset.org/10012619.pdf

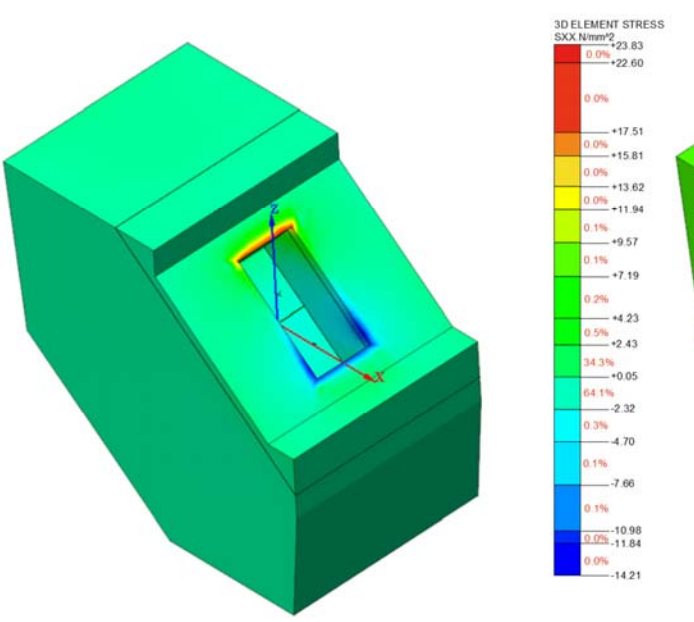

(a) Stress nephogram of longitudinal bridge

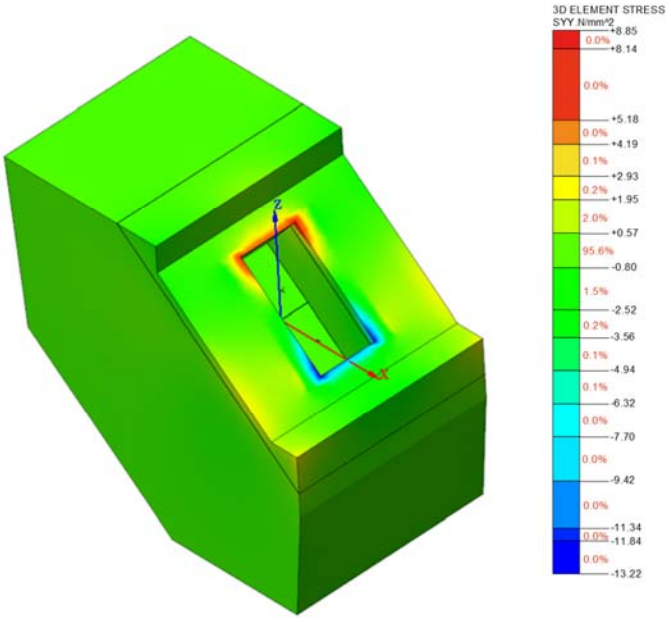

(b) Cross-bridge stress nephogram

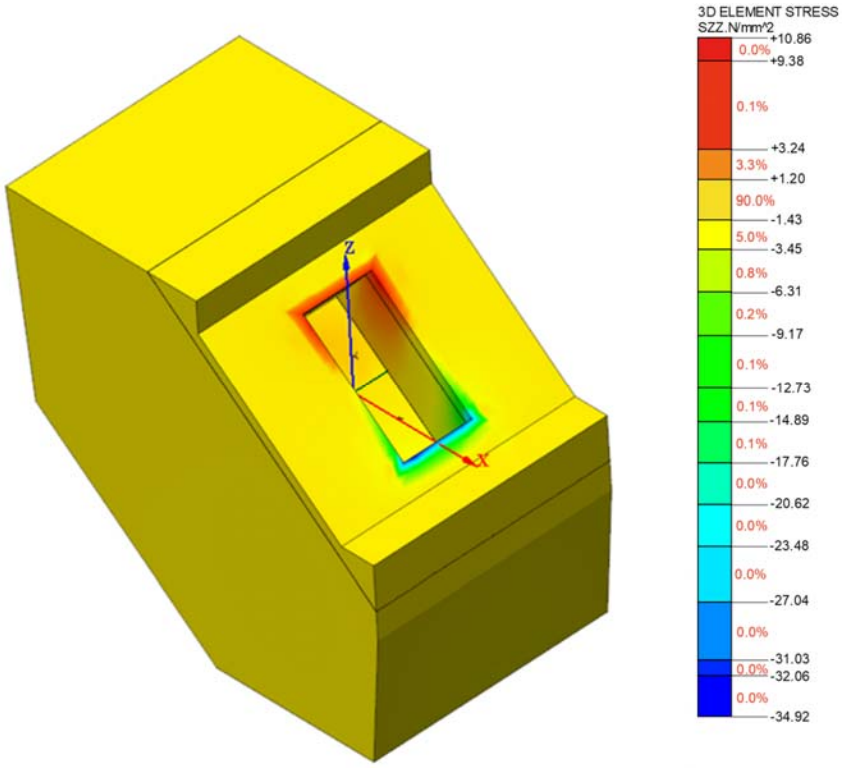

(c) Vertical stress nephogram

Fig. 4 Force of arch foot under working condition 2

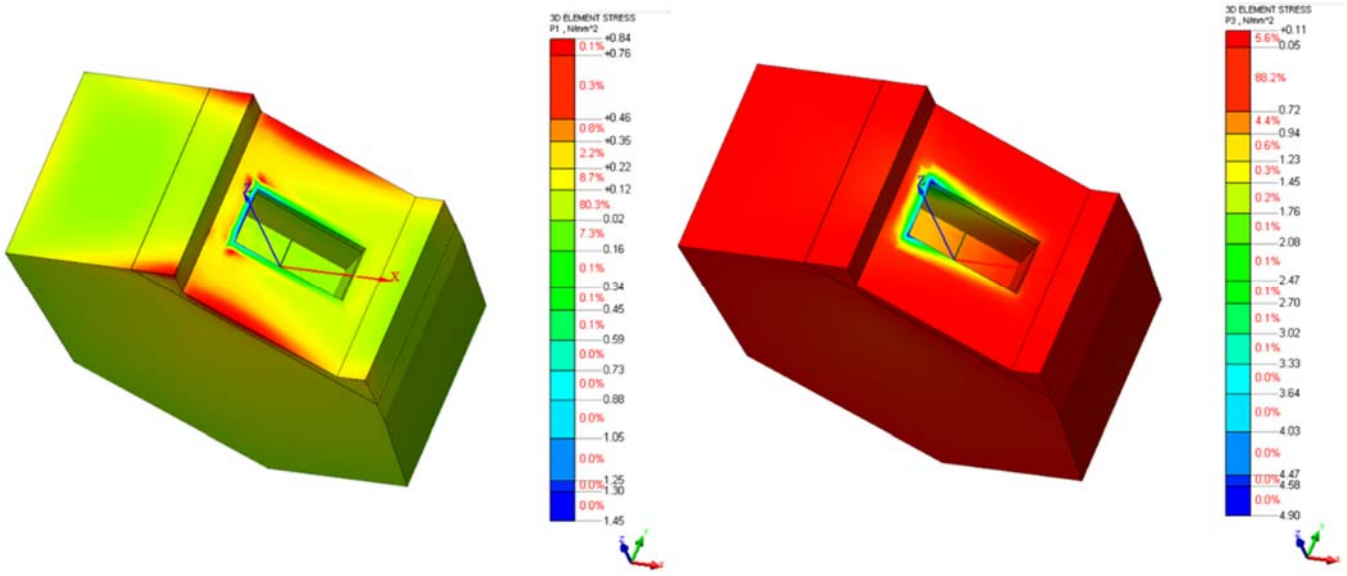

(a) Main tensile stress nephogram (b) Main pressure stress nephogram

Fig. 5 Principal stress under condition 1

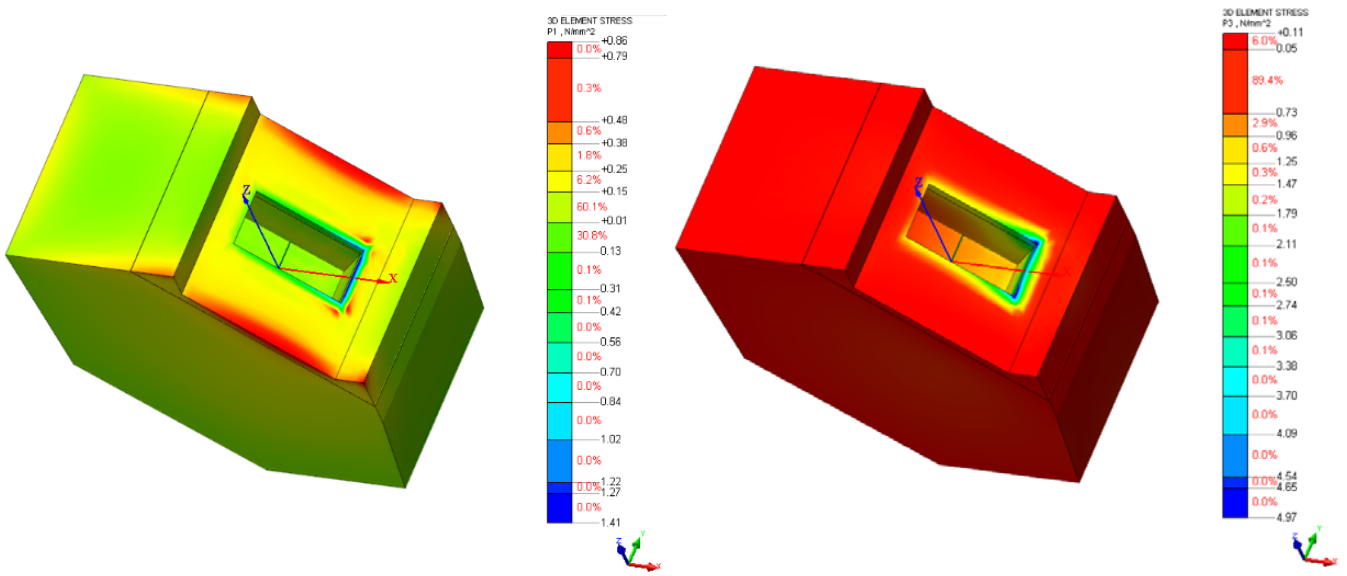

(a) Main tensile stress nephogram (b) Main pressure stress nephogram

Fig. 6 Principal stress under condition 2

IV. Discussion

Since the model does not consider the slip of concrete and arch steel plate, the tensile stress exceeds the limit at the interface between the two, but this part of the concrete accounts for a very small proportion, up to 2%. The stress of other parts meets the requirements.

V. Conclusions

1. In case of working condition 1, the stress of arch foot is mainly affected by longitudinal bridge direction.
2. Under working conditions 2 and 3, the vertical stress of arch foot is relatively large, and it is hardly affected by the transverse bridge direction.
3. The local analysis of arch foot shows that the stress of arch foot meets the specification requirements, and there is a slight stress concentration at the connection between arch rib and arch foot.

Open Science Index, Structural and Construction Engineering Vol:16, No:8, 2022 publications.waset.org/10012619.pdf

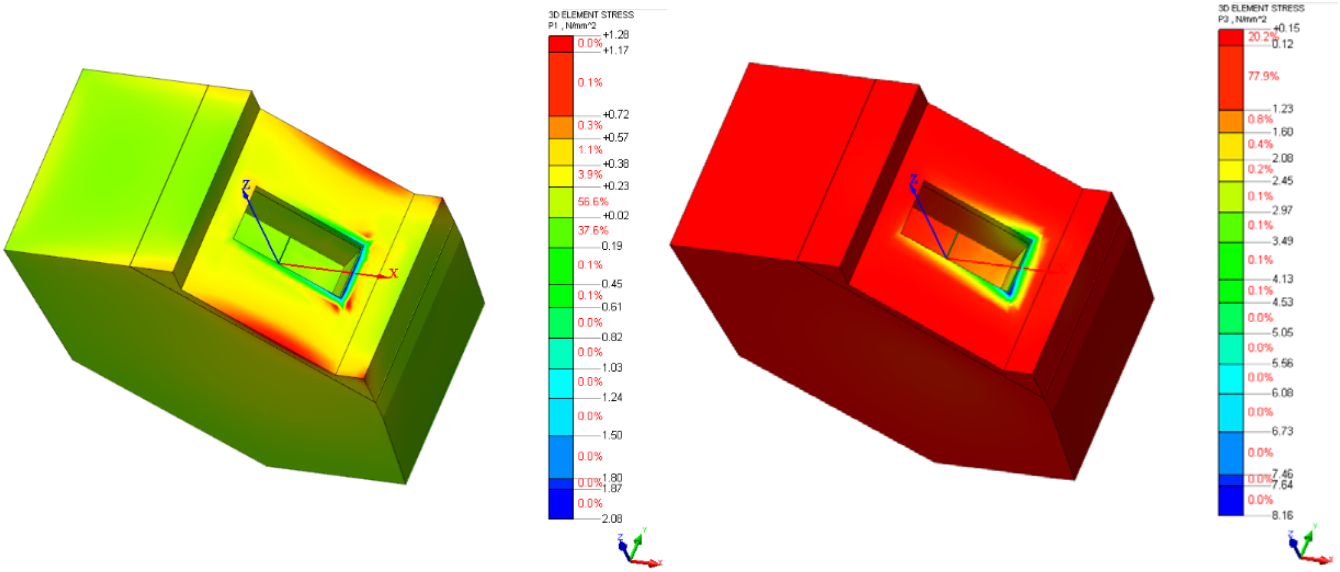

(a) Main tensile stress nephogram (b) Main pressure stress nephogram

Fig. 7 Principal stress under condition 3

REFERENCES

[1] Jia-Bo Xu, Zong-Lin W, Jia-Wei Xu. Stress Analysis of Girder of through Steel-box Tie-bar Arch-bridge (J). Science Technology and Engineering. 2011, 11(7): 1620-1622, 1627.

[2] Shui-Rong G, Shui-Sheng C, Shui W. Full-Scale Model Test Study of Load-Carrying Behavior of Hanger Joint of Tied Arch Bridge (J). Bridge Construction. 2013, 43(2): 58-63.

[3] Wang Xiao-ming, Yuan Yuan-yuan, Hao Xian-wu. Mechanical performance analysis and optimization of RC tied arch bridge arch rib suspender anchorage structure (J). Railway Engineering. 2013(07): 8-9.

[4] Li W, Kang J. Research on arch-beam joint analysis of inclined arch bridge (J). Highway. 2017, 62(7): 162-165.

[5] Ruan Bo. Finite Element Analysis of Local Complex Nodes of Xijiang Fourth Bridge in Wuzhou, Guangxi (J). Western Traffic Technology 2019(10): 69-72, 202.

[6] Liu An-xing. Mechanical properties analysis of a large span steel box basket arch bridge (J). Highway. 2020, 65(3): 121-126.

[7] Li Ke, Wang Qi, Zheng Ai-Hua. Large-span steel arch bridge cable arch and cable beam connection structure design and local stress analysis (J). Sichuan architecture. 2022, 42(02): 107-109.

Open Science Index, Structural and Construction Engineering Vol:16, No:8, 2022 publications.waset.org/10012619.pdf